



The University of
Nottingham

UNITED KINGDOM · CHINA · MALAYSIA

Cherns, D. and Webster, R. F. and Novikov, S. V. and Foxon, C. Thomas and Fischer, A. M. and Ponce, F. A. and Haigh, S. J. (2014) Compositional variations in In_{0.5}Ga_{0.5}N nanorods grown by molecular beam epitaxy. *Nanotechnology*, 25 (21). 215705/1-215705/6. ISSN 1361-6528

Access from the University of Nottingham repository:

http://eprints.nottingham.ac.uk/34758/1/Nanotechnology_2014_25_21_215705.pdf

Copyright and reuse:

The Nottingham ePrints service makes this work by researchers of the University of Nottingham available open access under the following conditions.

This article is made available under the Creative Commons Attribution licence and may be reused according to the conditions of the licence. For more details see:

<http://creativecommons.org/licenses/by/2.5/>

A note on versions:

The version presented here may differ from the published version or from the version of record. If you wish to cite this item you are advised to consult the publisher's version. Please see the repository url above for details on accessing the published version and note that access may require a subscription.

For more information, please contact eprints@nottingham.ac.uk

Compositional variations in $\text{In}_{0.5}\text{Ga}_{0.5}\text{N}$ nanorods grown by molecular beam epitaxy

This content has been downloaded from IOPscience. Please scroll down to see the full text.

View [the table of contents for this issue](#), or go to the [journal homepage](#) for more

Download details:

IP Address: 128.243.84.233

This content was downloaded on 04/06/2014 at 09:24

Please note that [terms and conditions apply](#).

Compositional variations in $\text{In}_{0.5}\text{Ga}_{0.5}\text{N}$ nanorods grown by molecular beam epitaxy

D Cherns¹, R F Webster¹, S V Novikov², C T Foxon², A M Fischer³,
F A Ponce³ and S J Haigh⁴

¹School of Physics, University of Bristol, Tyndall Avenue, Bristol BS8 1TL, UK

²Department of Physics and Astronomy, University of Nottingham, Nottingham NG7 2RD, UK

³Department of Physics, Arizona State University, Tempe, Arizona 85287-1504, USA

⁴Materials Science Centre, University of Manchester, Manchester M13 9PL, UK, and SuperSTEM Laboratory, Keckwick Lane, Daresbury, WA4 4AD, UK

E-mail: d.cherns@bristol.ac.uk

Received 11 February 2014, revised 25 March 2014

Accepted for publication 31 March 2014

Published 2 May 2014

Abstract

The composition of $\text{In}_x\text{Ga}_{1-x}\text{N}$ nanorods grown by molecular beam epitaxy with nominal $x=0.5$ has been mapped by electron microscopy using Z -contrast imaging and x-ray microanalysis. This shows a coherent and highly strained core-shell structure with a near-atomically sharp boundary between a Ga-rich shell ($x \sim 0.3$) and an In-rich core ($x \sim 0.7$), which itself has In- and Ga-rich platelets alternating along the growth axis. It is proposed that the shell and core regions are lateral and vertical growth sectors, with the core structure determined by spinodal decomposition.

Keywords: InGaN nanorods, transmission electron microscopy, molecular beam epitaxy, EDX mapping, core-shell structures, spinodal decomposition


(Some figures may appear in colour only in the online journal)

Introduction

Blue and blue-green light emitting diodes (LEDs) based on GaN/ $\text{In}_x\text{Ga}_{1-x}\text{N}$ quantum-well structures ($x < 0.2$) are commercially well established [1]. However, $\text{In}_x\text{Ga}_{1-x}\text{N}$ maintains the hexagonal wurtzite structure throughout its composition range, and has a direct bandgap ranging from 3.4 eV ($x=0$) to 0.7 eV ($x=1$), which covers the visible spectrum. This has led to great interest in producing GaN/ $\text{In}_x\text{Ga}_{1-x}\text{N}$ LEDs which work efficiently at higher In content, i.e. at longer wavelengths [2], as well as higher In content alloys for applications such as solar cells [3]. However, the efficiency of these devices falls significantly as the In content increases. This reflects a combination of factors, which

include decreasing material quality, due to high densities of threading and point defects, and reduced radiative recombination of carriers due to high internal electric fields which result from growth of strained InGaN layers on the polar {0001} planes in GaN [4, 5]. One solution has been to grow (0001)-oriented nanorod arrays, which have few or no defects, and to use these arrays either as a precursor for low defect-density overlayers [6], or as a basis for nanorod LEDs [7]. An alternative approach has been to grow field-free devices on the non-polar sidewalls of nanorods, generating 3D LEDs [8].

To facilitate these advances, the growth of $\text{In}_x\text{Ga}_{1-x}\text{N}$ nanorod arrays with high In content is of interest. However, the growth of alloy nanorods is inherently complicated as we need to consider growth on at least two surfaces, the polar (0001) and non-polar {10-10} side facets, where the mobility and desorption rates of In and Ga may differ. In addition, it is known that $\text{In}_x\text{Ga}_{1-x}\text{N}$ is thermodynamically unstable, owing

 Content from this work may be used under the terms of the Creative Commons Attribution 3.0 licence. Any further distribution of this work must maintain attribution to the author(s) and the title of the work, journal citation and DOI.

to the large difference in lattice parameter between GaN ($a=0.319$ nm, $c=0.519$ nm) and InN ($a=0.354$ nm, $c=0.570$ nm) [9]. Phase separation or spinodal decomposition should be suppressed in thin films owing to elastic constraints, but has been reported for high In content layers [10]. However, decomposition is more likely in nanostructures, where elastic relaxation is possible, and has been observed recently in Stranski–Krastanov islands [11, 12].

Studies of the growth of $\text{In}_x\text{Ga}_{1-x}\text{N}$ nanorods have suggested that growth is indeed complex. There is evidence of compositional variations both in the radial direction and parallel to the growth axis. Cai *et al* [13] reported that $\text{In}_x\text{Ga}_{1-x}\text{N}$ nanorods grown by chemical vapour deposition had a Ga-rich shell and an In-rich core; they proposed this resulted from spontaneous phase segregation. Similar core-shell structures have also been reported in GaN/ $\text{In}_x\text{Ga}_{1-x}\text{N}$ nanorods by several groups, although the interpretation is complicated by the additional in-plane mismatch strains, as well as possible migration of species between layers and changes in growth conditions. Tourbot *et al* [14] reported Ga-rich shells in GaN/ $\text{In}_x\text{Ga}_{1-x}\text{N}$ nanorods with an $\text{In}_x\text{Ga}_{1-x}\text{N}$ segment grown on a GaN nanorod base, and proposed that this depended on a combination of preferential absorption of Ga on the sidewalls and segregation of In on the [0001] growth surface to reduce mismatch strains. For nanorods grown in the [000-1] direction with GaN/ $\text{In}_x\text{Ga}_{1-x}\text{N}$ superlattices, Kehagias *et al* [15] found a limited In content in the core, and suggested that this resulted from reduced In incorporation on [000-1] facets compared with the surrounding semi-polar facets.

This paper uses compositional profiling in the scanning transmission electron microscope (STEM) to examine the growth of $\text{In}_{0.5}\text{Ga}_{0.5}\text{N}$ nanorods by plasma-assisted molecular beam epitaxy (PA-MBE). It is shown that the nanorods have a pronounced core-shell structure with a Ga-rich shell and In-rich core, with a near-atomically sharp boundary between the shell and core regions. The In-rich core is itself separated along the growth direction into alternating In-rich and In-poor regions. It is argued that the core-shell structure arises owing to growth on different facets, i.e. different growth sectors, and that the compositional variation in the core is due to phase separation.

Experimental

The $\text{In}_{0.5}\text{Ga}_{0.5}\text{N}$ nanorods were grown in a Varian ModGen II MBE system, with active nitrogen provided by an HD25 RF activated plasma source. Growth was carried out directly onto p-Si(111) substrates at substrate temperatures of 400–500 °C. These low substrate temperatures (which compare to about 800 °C for GaN growth) were required to reduce desorption of the more volatile In species. The substrate was rotated at 10 revolutions min^{-1} with the In and Ga sources inclined at equal angles $\sim 35^\circ$. The sample illustrated here was grown for 5 h under strongly N-rich conditions, i.e. with the active N flux much greater than the Ga and In fluxes. The RF power for the N-source was 450 W and the total N_2 flow was 2.5 sccm,

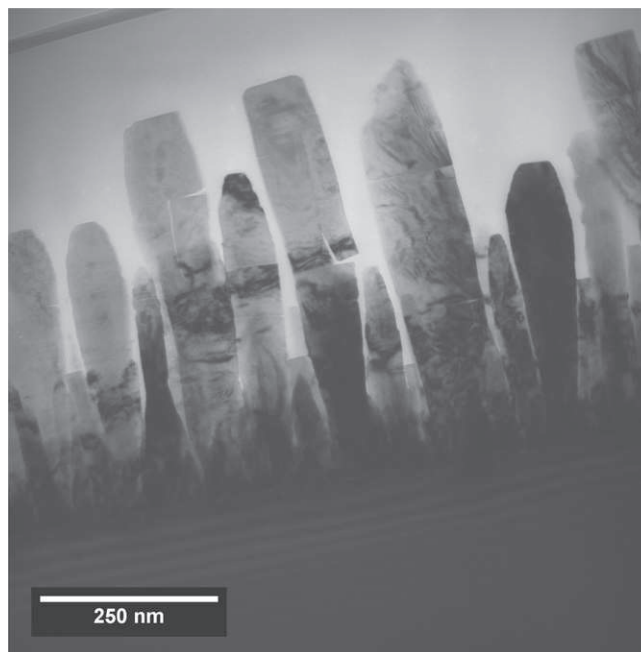


Figure 1. Bright field TEM image of a cross-sectional sample showing bend contours and cracks, but no threading dislocations.

which resulted in a nitrogen pressure in the MBE chamber of $\sim 4 \times 10^{-5}$ Torr. Beam equivalent pressures of In ($\sim 3.0 \times 10^{-8}$ Torr) and Ga ($\sim 2.2 \times 10^{-8}$ Torr) were used. Such fluxes produce approximately equal arrival rates for In and Ga adatoms taking into account the fact that the relative ion gauge sensitivities for In and Ga differ by 1.4:1.

Transmission electron microscopy (TEM) was carried out on cross-sectional samples prepared by mechanical polishing and Ar^+ ion thinning at 5 kV, with a final polish at 3 kV. Plan-view samples were also prepared by gluing together wafers using a conducting epoxy resin and cutting a thin section from the interfacial region using a dual-beam focussed ion beam microscope with Ga^+ ion thinning at 30 kV, followed by a final polish at 5 kV.

Results and interpretation

Figure 1 shows a bright field image of a cross-sectional sample taken at 200 kV in a Philips EM430 TEM. The nanorods show bend contours, but no evidence of threading dislocations. Some of the nanorods show cracks both on and perpendicular to the basal plane, a feature that was also observed on samples prepared by scraping nanorods directly onto a holey carbon film, suggesting that cracking is an inherent feature rather than a thinning artefact. Figures 2 and 3 show plan view and cross-sectional samples respectively, imaged by STEM in a Titan G2 ChemiSTEM microscope operated at 200 kV with probe current of 300 pA and a convergence angle of 21 mrad. High-angle-annular dark-field (HAADF) images and energy dispersive x-ray (EDX) maps were recorded in parallel, the latter using the ChemiSTEM's four silicon drift detectors with a total collection solid angle

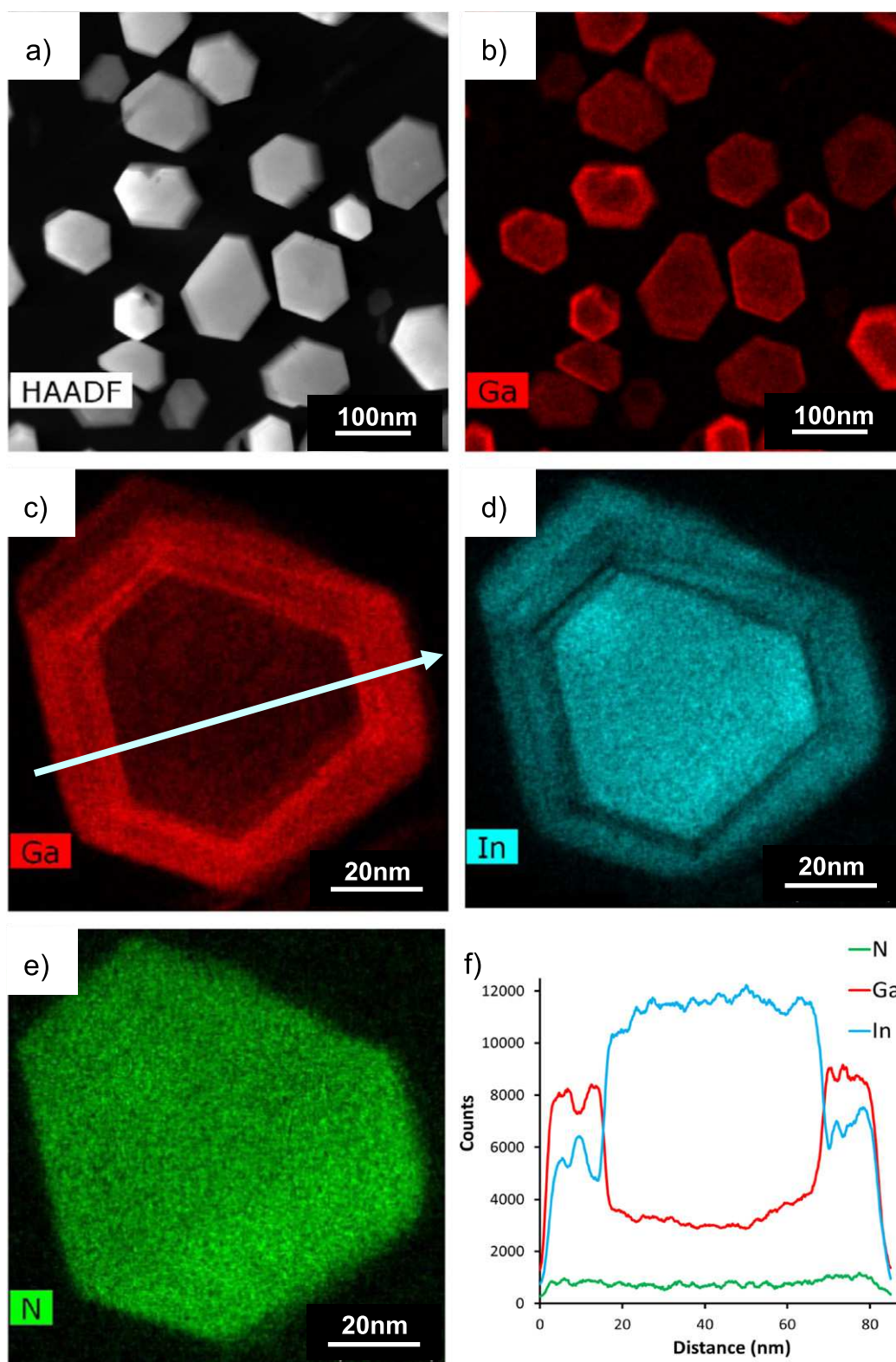


Figure 2. STEM on a plan-view sample: (a), (b) corresponding HAADF and Ga maps at low magnification, ((c)–(f)) Ga, In and N maps for a single nanorod section and a corresponding linescan showing elemental counts averaged over a 20 nm wide window in the arrowed direction.

of 0.7Sr. Quantification of EDX spectra was performed using a Cliff Lorimer approach within the Bruker ESPRIT software. Figure 2(a) shows a low magnification HAADF image of the plan-view sample, with a number of nanorod sections. There

is a pronounced $\{10\text{-}10\}$ faceting on the vertical side facets, which also reveals relative rotations between the nanorods, reflecting imperfect epitaxy on the (111)Si substrate. X-ray maps from around 20 nanorods showed that the majority had

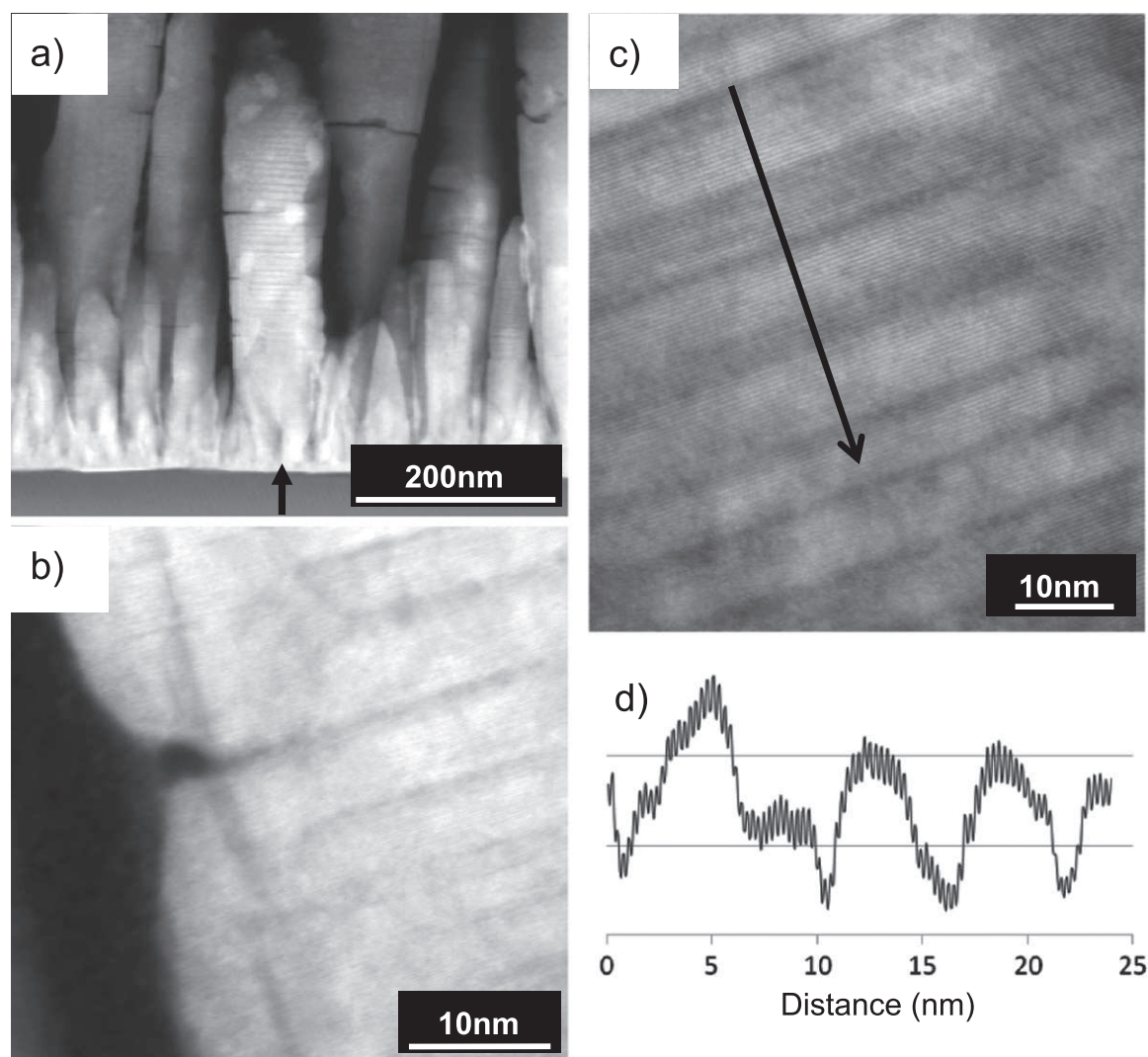


Figure 3. HAADF images of a cross-sectional sample: (a) general area view, (b) a crack which extends through the shell of one nanorod into a Ga-rich region in the core, (c) high magnification image of a core region, and (d) line trace of intensity along the arrow in (c).

a Ga-rich shell and an In-rich core. For example, figure 2(b) shows a Ga map corresponding to the area in figure 2(a). Figures 2(c)–(e) display the separate Ga, In and N maps for a single nanorod. Figure 2(f) shows line scans with a pixel size ~ 0.5 nm comparing x-ray counts along the arrowed direction in figure 2(c), corrected for absorption due to a film thickness of 25 nm measured by convergent beam electron diffraction. The line scans give average In compositions $x = 0.34 \pm 0.04$ and $x = 0.69 \pm 0.03$ for the shell and core respectively, and no change in the N content across the core-shell boundary. The results also suggest an extremely sharp boundary between the core and shell regions, with the apparent boundary width ~ 1 – 2 nm comparable to the spatial resolution of about 1 nm for the EDX maps, estimated by considering the interaction volume for a 25 nm thick sample and the convergence semi-angle of 21 mrad (ignoring electron channelling).

Figure 3 shows HAADF images of a cross-sectional sample. Considering the arrowed nanorod in figure 3(a), as a typical example from observations of more than 20 nanorods, the core region shows bright and dark bands alternating along

[0001] with a period of around 6 nm. In contrast, the shell shows uniform contrast. As HAADF images show contrast due predominantly to inelastic scattering, with intensity varying approximately as Z^2 , where Z is the atomic number, the brighter bands correspond to regions richer in In. This was confirmed by EDX mapping, although quantitative measurements of the Ga/In ratio in the core were not possible owing to the sandwich nature of the sample. Figures 3(b), (c) show higher magnification images. Figure 3(b) illustrates a surface crack which has extended into a Ga-rich region in the core. Figure 3(c) shows 0.27 nm fringes corresponding to the (0002) planes more clearly. These are the fine scale oscillations in the corresponding intensity line profile (figure 3(d)), which indicates that the boundaries between In-rich and Ga-rich regions are no wider than 1 nm.

The growth of nanorods in catalyst-free conditions, as here, is still uncertain. It is widely believed that the very N-rich conditions help to bond Ga and the more volatile In, and that adatom diffusion from the sidewalls to the (0001) surface promotes fast vertical growth. However, an alternative

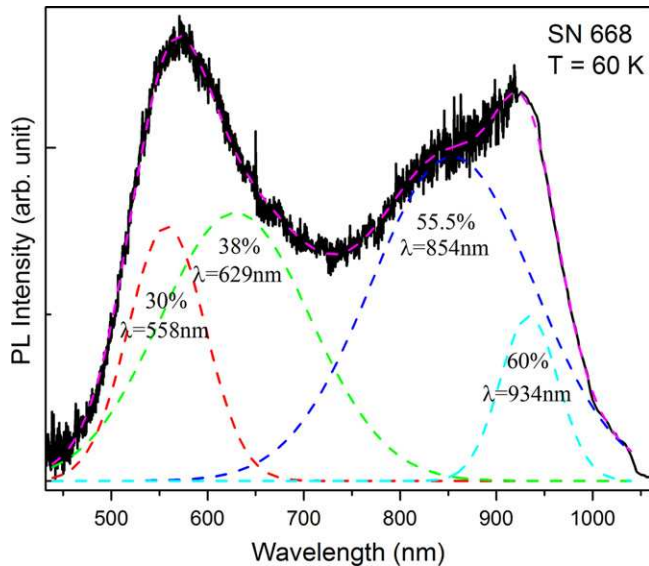


Figure 4. PL at 60 K and 200 μm spot size, corrected for response of the detectors, a Si CCD below 900 nm and Ge photodiode for longer wavelengths. A four-Gaussian fit to the spectrum is shown with each Gaussian labelled by the peak wavelength and the equivalent In content (%).

geometrical model, which explains the MBE growth of GaN nanorods, assumes no diffusion, or desorption, giving an aspect ratio which depends on the angle of inclination of the metal sources [16]. The results here throw new light on the growth mechanism. The sharp boundary between the shell and core, and the fact that the shell does not show structural changes along [0001], strongly suggests that it is a lateral growth sector. In figure 2, the In concentration in the shell (34%) is lower than expected from the adatom arrival rate (50% In, 50% Ga), suggesting an increased loss of In on the non-polar facets due to desorption or migration to the top surface. However, the average In concentration in the core (69%) is also greater than expected. This implies that there is a net influx of In from the sidewalls to the top surface.

The possibility that composition modulations in the core are related to periodic fluctuations in In or Ga flux during sample rotation in the growth chamber can be discounted, as the growth rate along [0001], ~ 0.2 nm per revolution, is much less than the modulation period (6 nm). Instead these modulations can be explained by spinodal decomposition. The general observation was that compositional modulations extended to the (0001) top surface of the nanorods, and thus probably formed at or close to the growth surface rather than during subsequent annealing. The phase diagram suggests that, without strain, decomposition should be into near phase pure GaN and InN [17]. Layer strains should reduce this composition difference, as shown using density functional theory [18, 19]. For example, Gan [18] gives 80% In, 7% In as the two spinodal compositions at 500 $^{\circ}\text{C}$. More insight into the composition of the core can be obtained by photoluminescence (PL). Figure 4 shows a PL spectrum recorded at 60 K and corrected for detector response. The spectrum up to 900 nm was recorded using a 325 nm HeCd laser and Si CCD

detector and above 900 nm (lower noise region) using a 532 nm Ti-sapphire laser with Ge photodiode detector. The spectrum shows two very broad peaks with maxima at about 570 nm and 930 nm, which can be tentatively ascribed to band edge recombination in regions of different composition. Ignoring localization and strain effects, the main peak maxima correspond to In content $x=0.31$ (570 nm) and $x=0.60$ (930 nm), consistent with recombination in the shell and in the core respectively. For the core, the scale of the compositional fluctuations is comparable to the exciton Bohr radius ~ 3 nm [20], implying that the PL is dominated by carrier migration to, and subsequent recombination in, the regions of highest In content, i.e. regions with the lowest band energy. The PL emission extends to about 1000 nm in the long wavelength limit, which gives an upper limit for the In content of about $x=0.69$. Given that there should be little carrier recombination associated with the Ga-rich platelets, it is not possible to directly use the shorter wavelength PL emission to gain information on their In content. However, the contrast of the Ga-rich platelets, as seen in HAADF images, is generally lower than that in the remaining core and shell regions, implying that the In content is probably less than that in the shell. Hence, taking the lower limit of around 500 nm in the PL emission as due to the shell, we can tentatively place an upper limit on the In content of $x=0.23$ for the Ga-rich platelets.

The fact that the nanorods are free of mismatch defects shows that they are under considerable mismatch strain. Given that the lattice parameters of InN and GaN differ by about 10% both in and perpendicular to the basal plane, the average mismatch between the core and shell regions in figure 2 is about 3.7%. As the volume ratio $V_{\text{shell}}:V_{\text{core}}$ is around 1.5, this is shared between tensile strain in the shell and compressive strain in the core, such that the maximum strain (in the core in this case) is about 2.2%. This differs for different nanorods as both the composition profile, and $V_{\text{shell}}:V_{\text{core}}$, differ significantly (see figure 2(b)). As the shell is under tensile stress, cracks will tend to propagate from the surface. In the absence of surface defects, this requires the tensile stress to be comparable with the theoretical strength, equivalent to roughly a 10% strain, but much lower at surface irregularities owing to stress concentration [21]. Once formed, cracks should, as observed, tend to extend beyond the shell into the Ga-rich platelets in the core which should be under tension with respect to the shell.

Conclusions

In summary, the results throw new light on the growth of $\text{In}_{0.5}\text{Ga}_{0.5}\text{N}$ nanorods by low temperature MBE, showing clearly that there are both lateral and vertical growth sectors where the rates of incorporation of In and Ga are different. There is also clear evidence of spinodal decomposition in the In-rich core into alternate In-rich and Ga-rich regions. Estimates of the compositions in these regions are consistent with the equilibrium phase diagram. More generally, our results suggest that a core-shell growth mode should occur over a

range of compositions, including perhaps the binaries, GaN and InN. With devices in mind, this implies further that incorporation of dopants as well as alloy species may differ in the shell and core regions.

Acknowledgements

This work is supported by the Engineering and Physical Sciences Research Council (EPSRC) under grant no. EP/I035501/1, and the NSF Materials World Network under grant NSF CA No. DMR-1108450.

References

- [1] Ponce F A and Bour D P 1997 *Nature* **386** 351
- [2] Crawford M G 2009 *IEEE J. Sel. Top. Quantum Electron.* **15** 1028–40
- [3] Wu J, Walukiewicz W, Yu K M, Shan W, Ager J W III, Haller E E, Lu H, Schaff W J, Metzger W K and Kurtz S 2003 *J. Appl. Phys.* **94** 6477
- [4] Cherns D, Barnard J and Ponce F A 1999 *Solid State Commun.* **111** 281
- [5] Ponce F A, Srinivasan S, Bell A, Geng L, Liu R, Stevens M, Cai J, Omiya H, Marui H and Tanaka S 2003 *Phys. Status Solidi B* **240** 273
- [6] Cherns D, Meshi L, Griffiths I, Khongphetsak S, Novikov S V, Farley N, Campion R P and Foxon C T 2008 *Appl. Phys. Lett.* **92** 121902
- [7] Lin H-W, Lu Y-L, Chen H-Y, Lee H-M and Gwo S 2010 *Appl. Phys. Lett.* **97** 073101
- [8] Waag A 2011 *Phys. Status Solidi C* **8** 2296
- [9] Teke A and Morkoc H 2006 *Springer Handbook of Electronic and Photonic Materials* ed S Kasap and P Capper (Berlin: Springer) p 757 (chapter 32)
- [10] Singh R, Doppalapudi D, Moustakas T D and Romano L T 1997 *Appl. Phys. Lett.* **70** 1089
- [11] Niu X, Stringfellow G B and Liu F 2011 *Appl. Phys. Lett.* **99** 213102
- [12] Tessarek C, Figge S, Aschenbrenner T, Bley S, Rosenauer A, Seyfried M, Kalden J, Sebald K, Gutowski J and Hommel D 2011 *Phys. Rev. B* **83** 115316
- [13] Cai X M, Leung Y H, Cheung K Y, Tam K H, Djuricic A B, Xie M H, Chen H Y and Gwo S 2006 *Nanotechnology* **17** 2330
- [14] Tourbot G, Bougerol C, Grenier A, Den Hertog M, Sam-Giao D, Cooper D, Gilet P, Gayrol B and Daudin B 2011 *Nanotechnology* **22** 075601
- [15] Th Kehagias *et al* 2013 *Nanotechnology* **24** 435702
- [16] Foxon C T, Novikov S V, Hall J L, Campion R P, Cherns D, Griffiths I and Khongphetsak S 2009 *J. Cryst. Growth* **311** 3423
- [17] Ho I and Stringfellow G B 1996 *Appl. Phys. Lett.* **69** 2701
- [18] Karpov S Y, Podolskaya N I, Zhmakin I A and Zhmakin A I 2004 *Phys. Rev. B* **70** 235203
- [19] Gan C K, Feng Y P and Srolovitz D J 2006 *Phys. Rev. B* **73** 235214
- [20] Ramvall P, Tanaka S, Nomura S, Riblet P and Aoyagi Y 1998 *Appl. Phys. Lett.* **73** 1104
- [21] Lawn B 1993 *Fracture of Brittle Solids* 2nd edn (Cambridge: Cambridge University Press)